

2-8-2021

Cerebral endothelial cell-derived small extracellular vesicles enhance neurovascular function and neurological recovery in rat acute ischemic stroke models of mechanical thrombectomy and embolic stroke treatment with tPA

Chao Li

Henry Ford Health, CL11@hfhs.org

Chunyang Wang

Henry Ford Health, CWang2@hfhs.org

Yi Zhang

Henry Ford Health, yzhang3@hfhs.org

Owais K. Alsrouji

Henry Ford Health, oalsrou1@hfhs.org

Alex B. Chebl

Henry Ford Health, achebl1@hfhs.org

See next page for additional authors

Follow this and additional works at: https://scholarlycommons.henryford.com/neurology_articles

Recommended Citation

Li C, Wang C, Zhang Y, Alsrouji OK, Chebl AB, Ding G, Jiang Q, Mayer SA, Lu M, Kole MK, Marin HL, Zhang L, Chopp M, and Zhang ZG. Cerebral endothelial cell-derived small extracellular vesicles enhance neurovascular function and neurological recovery in rat acute ischemic stroke models of mechanical thrombectomy and embolic stroke treatment with tPA. J Cereb Blood Flow Metab 2021.

This Article is brought to you for free and open access by the Neurology at Henry Ford Health Scholarly Commons. It has been accepted for inclusion in Neurology Articles by an authorized administrator of Henry Ford Health Scholarly Commons.

Authors

Chao Li, Chunyang Wang, Yi Zhang, Owais K. Alsrouji, Alex B. Chebl, Guangliang Ding, Quan Jiang, Stephan A. Mayer, Mei Lu, Max K. Kole, Horia L. Marin, Li Zhang, Michael Chopp, and Zhenggang Zhang

Cerebral endothelial cell-derived small extracellular vesicles enhance neurovascular function and neurological recovery in rat acute ischemic stroke models of mechanical thrombectomy and embolic stroke treatment with tPA

Journal of Cerebral Blood Flow & Metabolism

0(0) 1–15

© The Author(s) 2021

Article reuse guidelines:

sagepub.com/journals-permissions

DOI: 10.1177/0271678X21992980

journals.sagepub.com/home/jcbfm



Chao Li¹ , Chunyang Wang¹, Yi Zhang¹, Owais K Alsrouji¹, Alex B Chebl¹, Guangliang Ding¹, Quan Jiang¹, Stephan A Mayer², Mei Lu³, Max K Kole⁴, Horia L Marin⁵, Li Zhang¹, Michael Chopp^{1,6} and Zheng Gang Zhang¹

Abstract

Treatment of patients with cerebral large vessel occlusion with thrombectomy and tissue plasminogen activator (tPA) leads to incomplete reperfusion. Using rat models of embolic and transient middle cerebral artery occlusion (eMCAO and tMCAO), we investigated the effect on stroke outcomes of small extracellular vesicles (sEVs) derived from rat cerebral endothelial cells (CEC-sEVs) in combination with tPA (CEC-sEVs/tPA) as a treatment of eMCAO and tMCAO in rat. The effect of sEVs derived from clots acquired from patients who had undergone mechanical thrombectomy on healthy human CEC permeability was also evaluated. CEC-sEVs/tPA administered 4 h after eMCAO reduced infarct volume by ~36%, increased recanalization of the occluded MCA, enhanced cerebral blood flow (CBF), and reduced blood-brain barrier (BBB) leakage. Treatment with CEC-sEVs given upon reperfusion after 2 h tMCAO significantly reduced infarct volume by ~43%, and neurological outcomes were improved in both CEC-sEVs treated models. CEC-sEVs/tPA reduced a network of microRNAs (miRs) and proteins that mediate thrombosis, coagulation, and inflammation. Patient-clot derived sEVs increased CEC permeability, which was reduced by CEC-sEVs. CEC-sEV mediated suppression of a network of pro-thrombotic, -coagulant, and -inflammatory miRs and proteins likely contribute to therapeutic effects. Thus, CEC-sEVs have a therapeutic effect on acute ischemic stroke by reducing neurovascular damage.

Keywords

Acute ischemic stroke, blood-brain barrier, small extracellular vesicles, tPA, endothelial cells

Received 21 October 2020; Revised 9 January 2021; Accepted 11 January 2021

Introduction

Stroke is the fifth leading cause of death and the leading cause of disability worldwide. Cerebral large vessel occlusion is the most disabling and life-threatening cause of ischemic stroke.^{1,2} Approximately two-thirds of eligible patients treated with tissue plasminogen activator (tPA) experience incomplete brain reperfusion.³ Mechanical thrombectomy performed within 24 hours of stroke onset is now also the standard of care for the treatment of acute ischemic stroke with large vessel

¹Department of Neurology, Henry Ford Health System, Detroit, MI, USA

²Departments of Neurology and Neurosurgery, Westchester Medical Center, New York Medical College, Valhalla, NY, USA

³Department of Biostatistics and Research Epidemiology, Henry Ford Health System, Detroit, MI, USA

⁴Department of Neurological Surgery, Henry Ford Health System, Detroit, MI, USA

⁵Clinical Professor of Radiology, Wayne State University School of Medicine, Detroit, MI, USA

⁶Department of Physics, Oakland University, Rochester, MI, USA

Corresponding author:

Zheng Gang Zhang, Department of Neurology in Henry Ford Hospital, 2799 West Grand Blvd. Detroit, MI 48202, USA.

Email: ZZhang1@hfhs.org

occlusion.^{1,2,4–8} Reperfusion of the ischemic penumbra is closely associated with good clinical outcomes.^{1,2} Although recanalization of the large vessel occlusion by thrombectomy is achieved in >71% of patients, it is often incomplete, and ~50–52% of patients achieve good neurological outcomes.^{1,2,4–6,9} Moreover, many patients with large vessel occlusion exhibit rapid expansion of the ischemic core during the first few hours, which leads to unfavorably large ischemic cores and are not eligible to receive tPA or endovascular therapy. Thus, there is a compelling need to develop therapies in combination with tPA and thrombectomy to enhance cerebral perfusion and augment therapeutic efficacy. Also, therapies to block ischemic core expansion will increase the number of patients who would be eligible to receive tPA and thrombectomy.

Small extracellular vesicles (sEVs) including exosomes are endosomal origin membranous nanovesicles that mediate intercellular communication by transferring cargo proteins, lipids, and genomic materials including microRNAs (miRs) between source and recipient cells.^{10,11} Our group was the first to demonstrate that exosomes derived from mesenchymal stromal cells given to rats 24 h after middle cerebral artery occlusion (MCAO) substantially promote functional recovery by exosomal miR-mediated brain remodeling processes; however, these exosomes did not reduce cerebral infarction.^{12–14} Others have subsequently shown that treatment of acute stroke in animals with sEVs derived from human neural stem cells or human cardiosphere-derived cells alone or in combination with tPA, respectively, reduces infarction and improves functional outcomes.¹⁵ However, the therapeutic effect of sEVs on acute stroke in particular in ischemic stroke with large artery occlusion remains to be investigated.

Using rat models of embolic MCAO (eMCAO) and transient MCAO (tMCAO, ischemia/reperfusion), both of which mimic patients with a large artery occlusion,^{12,27–29} the present study investigated the effect of sEVs derived from human cerebral endothelial cells (CEC-sEVs) in combination with tPA (CEC-sEVs/tPA) and as co-therapy with mechanical reperfusion on acute ischemic stroke, respectively. Our data indicate that CEC-sEVs/tPA given acutely after the onset of eMCAO, or CEC-sEVs given upon reperfusion after tMCAO substantially increase recanalization of the embolic-occluded MCA and enhance downstream cerebral blood flow (CBF), and reduce blood-brain barrier (BBB) leakage after eMCAO and significantly reduce cerebral infarction and improve neurological outcomes in both eMCAO and tMCAO stroke models compared with their respective controls. Moreover, CEC-sEVs administered intravenously cross the BBB and are

preferentially internalized by cerebral endothelial cells, astrocytes, and neurons in the ischemic hemisphere.

Material and methods

All animal experimental procedures were approved by the Institutional Animal Care and Use Committee (IACUC) of Henry Ford Hospital in accordance with the standards for humane animal care and use as set by the Animal Welfare Act (AWA), the National Institute of Health Guide for the Care and Use of Laboratory Animals and ARRIVE (Animal Research: Reporting in Vivo Experiments). Cerebral arterial clots were acquired from patients with acute ischemic stroke who underwent endovascular thrombectomy under an Institutional Review Board (IRB) protocol approved by the Institutional Review Board committee of Henry Ford Hospital and adhered to the principles of the Declaration of Helsinki (2008). All participants were provided with an information sheet and all procedures were verbally explained in detail. All participants gave written informed consent after having the opportunity to ask questions and receive appropriate clarification. All experiments and outcome assessments were performed by observers blinded to the treatments.

Isolation and characterization of sEVs from CECs and arterial clots

For isolation of CEC-sEVs: CEC-sEVs were isolated from the supernatant of cultured primary CECs harvested from healthy adult rats using differential ultracentrifugation according to the published protocol.¹⁶ Briefly, the supernatant was filtered through a 0.22 µm filter (Millipore-Sigma, MO) to sieve out the dead cells and large growth debris. To remove additional debris, the filtered supernatant was centrifuged at 10,000×g for 30 minutes. Ultracentrifugation was then performed at 100,000×g for 3 hours to collect sEVs. The numbers and sizes of particles in the pellet were measured and analyzed using the nanoparticle tracking analyzer (NTA), NanoSight N300 System, (Merkel Technologies, Yehud, Israel). Morphology and protein markers of CEC-sEVs were examined using transmission electron microscopy (TEM) and Western blot, respectively. For isolation of human clot sEVs,¹⁷ patients with large vessel occlusion presenting within 24 hrs of acute ischemic stroke onset were treated with mechanical thrombectomy according to published guidelines.¹⁸ Those who qualified within 4.5 hours of onset were also treated with intravenous tPA. Mechanical thrombectomy was performed using an 8 French balloon guide catheter placed in the internal carotid artery or a 6 French guide catheter placed in

the vertebral artery. Clot retrieval was then performed utilizing a stent-retriever and proximal aspiration. If this approach failed after 2–3 attempts then distal aspiration was performed using a commercially available aspiration catheter often in combination with a stent-retriever. The retrieved clots were immediately placed in a fixative on ice and then stored in a refrigerator at 4°C. Cerebral arterial clots were homogenized within 12 h after the acquisition. Homogenization was centrifuged at 2,000 g for 15 mins and re-suspended in type3 collagenase (Rockland, PA) and protease inhibitors (S8820, Millipore-Sigma, MO) to dissociate tissue and to remove the remaining enzyme, respectively. Then, sEVs were isolated and characterized following the procedures used for CEC-sEVs.

Animal models

Male Wistar rats weighing 350–400 g and 275–300 g were subjected to eMCAO or tMCAO, respectively. Briefly, for eMCAO,¹⁹ a modified PE-50 catheter was introduced into the lumen of the right external carotid artery (ECA) through a small puncture. The catheter was gently advanced from the ECA into the lumen of the internal carotid artery (ICA) for 17–18 mm. A single clot (40 mm in length) was placed at the origin of the MCA via the catheter. For tMCAO (2 h),²⁰ a 4–0 monofilament nylon suture with its tip rounded by high heat, was advanced from the right ECA into the lumen of ICA for 18–19 mm until it blocked the origin of the MCA. Two hours after MCAO, reperfusion was achieved by withdrawal of the filament.

To acutely ascertain induction of stroke and in order to minimize animal stress by not performing detailed functional outcome measurements, the Longa five-point score was used to assay rat neurological deficits at 1 h after MCAO.²⁰ Rats with a score ≥ 2 were enrolled in the present study because we have demonstrated that animals with a score ≥ 2 have a substantial reduction of cerebral blood flow (CBF) in the MCA territory after MCAO induced by a clot or a filament.^{21–24}

Experimental protocol

To examine the effect of CEC-sEVs/tPA on acute ischemic stroke, rats subjected to eMCAO were randomly assigned to the following treatment groups: 1) CEC-sEVs alone, 2) tPA alone, 3) the combination of CEC-sEVs and tPA, and 4) Saline. (n = 10). CEC-sEVs (1×10^{11} particles/rat) were administered intravenously (IV) at 4 h and 24 h after MCAO. tPA (Genentech, San Francisco, CA) was infused intravenously at a dose of 10 mg/kg as a 10% bolus starting at 4 h after eMCAO, and the remainder was continuously infused over 30

mins. We have demonstrated that tPA alone given at 2 h, but not at 4 h, after eMCAO to adult rats has a therapeutic effect on acute embolic stroke.^{25,26} In the present study, to examine whether CEC-sEVs enhance tPA thrombolysis, a 4 h time point was selected. All rats were sacrificed at 7 days after eMCAO for measurements of infarct volume. Additional sets of rats were sacrificed at 26 h after eMCAO to assay residual clot mass, cerebral vascular perfusion, BBB leakage, and gross hemorrhage.²⁷

To examine whether early administration of CEC-sEVs reduces ischemic core expansion, CEC-sEVs (1×10^{11} particles/rat) were administered at 1 h after eMCAO via a tail vein and ischemic rats treated with saline were used as control (n = 6). The development of ischemic lesion was measured by means of MRI at 2 h and 24 h after stroke onset.

To examine whether CEC-sEVs reduce ischemic lesion, CEC-sEVs (1×10^{11} particles/rat) were administered via the internal carotid artery (IA) immediately following the withdrawal of the filament at 2 h after tMCAO (n = 6). A second dose of CEC-sEVs (1×10^{11} particles/rat) was administered at 24 h after tMCAO via a tail vein. Rats subjected to tMCAO treated with the same volume of saline were used as a control group (n = 6). All rats were sacrificed at 7 days after tMCAO for measurements of infarct volume.

Behavioral tests

An array of behavioral tests to measure sensorimotor function were performed at 1 day and 7 days after ischemia in both eMCAO and tMCAO models by observers blinded to the treatments. Modified neurological severity score (mNSS) is a composite of motor, sensory, reflex, and balance tests.²⁸ Neurological function was graded on a scale of 0 to 18 (normal score, 0; maximal deficit score, 18). The Adhesive removal test which records the mean time required to remove an adhesive paper from individual front paws provides an index of somatosensory deficits.²⁹ The Foot-fault test detects forelimb dysfunction³⁰ by measuring the total number of steps (movement of each forelimb) and the number of foot faults when the rat crossed the grid.

Magnetic resonance imaging (MRI) measurements

MRI measurements were performed with a 7-T preclinical MRI scanner (Bruker-Biospin, Billerica, MA). MRI measurements were performed at 1 h, 4.5–5 h, and 24 h after the onset of eMCAO, and included magnetic resonance angiography, perfusion-weighted imaging, apparent diffusion coefficient (ADC), and transverse relaxation time (T2).³¹ Ischemic lesion

volume was calculated by means of a threshold value of the mean ADC value with two times the standard deviation of the contralateral hemisphere tissue.³¹

Histopathologic analysis

To measure infarct volumes, rats at 7 days after eMCAO and tMCAO were sacrificed by transcardial perfusion with heparinized saline followed by 4% paraformaldehyde. Brains were removed and fixed in 4% paraformaldehyde. Infarct volume was measured on 7 hematoxylin and eosin (H&E) stained coronal sections using a Micro Computer Imaging Device (MCID) system, as previously described.¹⁹

To measure the residual embolus at the origin of occluded MCA, rats ($n=6$ /group) were sacrificed at 26 h after eMCAO by transcardial perfusion with saline and followed with 4% paraformaldehyde. The residual embolus at the origin of the MCA was imaged with a digital camera and the area of residual embolus (mm^2) was measured, as previously described with some modifications.²⁷ The present study directly measured the size of the entire residual embolus, while in our prior study, a residual pre-fluorescently labeled clot was measured.²⁷

Gross hemorrhage, defined by identification of blood accumulation in brain tissue with an unaided naked-eye was measured on H&E-stained coronal sections in rats sacrificed at 26 h after eMCAO.²⁷ The incidence of gross hemorrhage is presented as the percentage of rats with a visually identified gross hemorrhage in each experimental group ($n=6$ /group).

Measurement of plasma-perfused cerebral vessels

To measure blood plasma perfused cerebral blood vessels, fluorescein isothiocyanate (FITC)-dextran (2×10^6 molecular weight, Sigma, 50 mg/rat, IV) was administered to rats 26 h after eMCAO ($n=6$ /group). Rats were sacrificed 15 min after FITC-dextran injection and 3 coronal vibratome sections ($100 \mu\text{m}$ /section) obtained from the center of the ischemic lesion (bregma 0.2 to -0.8 mm) were analyzed using the MCID system, as previously described.²⁷ The area of FITC-dextran perfused blood vessels was measured and presented as the percentage of FITC-dextran perfused area within the territory supplied by the MCA.

Measurement of Evans blue extravasation

Parenchymal Evans blue extravasation was measured in rats 26 h after eMCAO, as previously described ($n=3$ /group).²⁷ Briefly, Evans blue (2% in saline; 1 ml/rats) was iv injected 24 h after eMCAO. Rats were transcardially perfused with saline at 2 h after

the injection. Each hemisphere was weighed, homogenized in 2 mL 50% trichloroacetic acid, and centrifuged. The fluorescence intensity in the supernatant was determined using a microplate fluorescence reader (excitation 620 nm and emission 680 nm). The amount of Evans blue within the ipsilateral hemisphere was quantified based on a standard curve generated with the external standards dissolved in the same solvent and is presented as $\mu\text{g/g}$ of tissue.

Immunohistochemistry and Western blot

Immunofluorescent staining was performed on coronal sections at the center of the ischemic lesion obtained from rats sacrificed at 26 h after eMCAO. Brain tissues were harvested from the peri-ischemic lesion including cortex and subcortex. The following primary antibodies were used: goat monoclonal antibody (mAb) against fibrinogen/fibrin (1:200, YNGRaFbg7S, Accurate Chemical & Scientific), mouse mAb against endothelial barrier antigen (EBA, 1:200, SMI71, Sternberger Monoclonals Inc), rabbit polyclonal antibody (pAb) anti-thrombocytes (1:200, CLA51440, Cedarlane). EBA immunoreactivity was used to identify cerebral blood vessels. For quantification, the numbers of vessels with fibrin/fibrinogen and thrombocytes immunoreactivity were counted throughout the territory supplied by the right MCA and are presented as the density of immunoreactive vessels relative to the scan area (mm^2).

Western blots were performed according to published methods.³² Briefly, equal amounts of total protein for each sample were loaded on 10% SDS-polyacrylamide gels. The blots were subsequently probed with the following primary antibodies: rabbit pAb against TLR2 or TLR4 (1:1,000, ab213676, or ab13556, Abcam), rabbit pAb against tissue factor (TF, 1:1,000, ab104513, Abcam), rabbit pAb against PAI-1 (1:1,000, ab66705, Abcam), rabbit pAb against P-selectin (1:1,000, PA5-87043, Invitrogen), rabbit pAb against HMGB1 (1:1,000, 3935 s, Cell Signaling Technology), rabbit pAb against CD63 (1:1,000, ab118307, Abcam), mouse mAb against Alix (1:1,000, MA1-83977, Thermo Fisher Scientific), rabbit mAb against ICAM-1 (1:1000, ab53013; Abcam), rabbit pAb against zonula occludin-1 (ZO1, 1:1,000, ab96587; Abcam), and rabbit mAb against phosphorylated NF (nuclear factor)- κB p65 at Ser536 (pp65 [phosphorylated p65], 1:1,000, 3033S; Cell Signaling Technology) and mouse mAb against β -actin (1:5,000, ab8226; Abcam). Western blots were performed from at least 3 individual experiments.

CEC integrity assay

Healthy human CECs were purchased from ScienCell (Cat#1,000; Carlsbad, CA). The endothelial monolayer barrier assay was performed according to our published method.³³ Briefly, endothelial cells (passage 2 to 4) were cultured for 7 days at a density of 5×10^4 per well and were then seeded as monolayer onto the inner chamber of trans-well insert (Corning). Small EVs were added into the culture medium for 48 h. Fluorescent-conjugated dextran (0.5 mg/mL, 70 kDa, D1830; Thermo Fischer Scientific) was then added to the top of the trans-wells for 30 minutes. Fluorescent signals in the bottom medium were then measured using a plate reader at excitation and emission wavelengths of 595 nm and 615 nm, respectively. Trans-endothelial permeability was calculated as % signals = (optical density experimental-optical density vehicle)/optical density vehicle $\times 100$. All data were obtained from 3 individual experiments.

Analysis of miRs and Bioinformatics analysis

miRs were isolated from rat primary CECs and CEC-sEVs by means of the miRNeasy Mini kit (Qiagen, Valencia, CA, USA) following the manufacturer protocol. Quantitative RT-PCR was performed on an ABI 7000 and ABI ViiATM 7 PCR instrument (Applied Biosystems, Foster City, CA). miRs were reversely transcribed with the miR Reverse Transcription kit (Applied Biosystems, Foster City, CA) and amplified with the TaqMan miR assay (Applied Biosystems, Foster City, CA), which is specific for mature miRNA sequences. U6 snRNA was used as an internal control. Analysis of gene expression was carried out by the $2^{-\Delta\Delta C_t}$ method. For the miR array, quality control of the total RNA samples was assessed using UV spectrophotometry and agarose gel electrophoresis. The samples were DNase digested and low-molecular-weight (LMW) RNA was isolated by ultra-filtration through YM-100 columns (Millipore, Billerica, MA) and subsequent purification using the RNeasy MinElute Clean-Up Kit (Qiagen, Valencia, CA). The LMW RNA samples were 3'-end-labeled with biotin dye using the FlashTagTM Biotin RNA Labeling Kits (Genisphere, Hatfield, PA). Labeled LMW RNA samples were hybridized to the MicroRNA microarrays according to conditions recommended in the Flash Taq RNA labeling Kit manual. The microarrays were scanned on an Axon Genepix 4000B scanner (Affymetrix Inc), and data were extracted from images using GenePix V4.1 software. miRNA QC Tool (Affymetrix Inc). Microarray data is MIAME compliant and the raw data have been deposited in the Gene Expression Omnibus database.

Ingenuity Pathway Analysis (IPA) software (QIAGEN; Hilden, Germany) was used for signaling pathway analysis. Gene and miR names were imported into IPA and processed using the core analysis tool. Using the IPA knowledge base, networks of experimental proteins and miRs were built. Networks were graphically visualized as hubs (proteins and miRs) and edges (the relationship between proteins and miRs).

GFP-CEC-sEVs construction and sEV distribution

To examine the distribution of intravenously administered CEC-sEVs in the ischemic brain, CEC-sEVs carrying CD63-GFP (GFP-sEVs) were generated according to our published protocols.³⁴ Briefly, CECs were transfected with a plasmid carrying pEGFP-CD63 vector (CD63-pEGFP C2, a gift from Paul Luzio, Addgene plasmid # 62964) by means of electroporation (Nucleofector system, program U11, Lonza). CD63 is a membrane protein marker of exosomes.³⁵ The presence of GFP proteins in sEVs (GFP-sEVs) was examined by means of Western blot.

To track the brain distribution of CEC-sEVs, immunogold based TEM imaging was used. Briefly, GFP-CEC-sEVs (3×10^{11} particles/mouse) were intravenously injected via a tail vein into the rat at 4 h after eMCAO ($n = 3$). Ischemic rats ($n = 3$) that received naïve-CEC-sEVs were used as a control. Two hours after the injection, the rat brain was collected and fixed by 2.5% glutaraldehyde in 0.1 M sodium cacodylate buffer for 24 hours at 4°C. The brain tissues were post-fixed by 1% Osmiumtetroxide/1.5% Potassium ferrocyanide for 1 hour at room temperature and embedded into the resin mixture. The ultrathin sections (85 nm) were obtained and mounted on nickel grids. Immunogold staining was then performed with a 2% anti-GFP rabbit monoclonal antibody (G10362, ThermoFisher) and 10 nm gold conjugated streptavidin (25,269 EMS). The grids were imaged under TEM (JEM-1400Flash, JEOL).

Statistical analysis

Sample size was determined based on our preliminary data which showed an effect size of 6.26 and 0.99 on 2 and 7 days infarction, respectively, between tPA alone and tPA in combination with CEC-sEVs. Considering $\alpha = 0.05$, a two-sided test, 10/group for 7 days and 6–8/group for earlier assessments, there is an 80% power to detect effect sizes of 1.48 and 1.68, respectively, assuming equal space of means.

Data were evaluated for normality by the Shapiro-Wilk test and ranked data were used for behavioral data analysis since the modified neurological severity

score data were not normally distributed. Using the intention-to-treat approach, if an animal died before the designated endpoint, the worse observed behavioral test score was used. The Global test using the Generalized Estimating Equation was implemented to test the treatment effect on the behavioral outcome measured from 3 behavioral tests at each time point. Additionally, statistical analysis was performed using the Statistical Package for the Social Sciences (SPSS, version 11.0; SPSS Inc, Chicago, IL). One-way ANOVA with post hoc Bonferroni tests was used when comparing more than two groups. The student's t-test was used when comparing two groups. All data are presented as mean \pm standard deviation. A p-value < 0.05 was considered significant.

Results

CEC-sEVs significantly reduce infarct volume and improve neurological outcomes in the rat

CEC-sEVs were isolated from the supernatant of cultured primary rat CECs using ultracentrifugation.¹⁶ We previously demonstrated that tPA alone given at 2 h, but not at 4 h, after eMCAO to adult rats has a therapeutic effect on acute stroke.^{25,26} To examine whether CEC-sEVs enhance the therapeutic effect of tPA given 4 h after eMCAO, CEC-sEVs (1×10^{11} particles/rat) in combination with tPA (10 mg/kg) were administered via a tail vein to adult male rats 4 h after eMCAO and a second dose of CEC-sEVs alone was given 24 h after eMCAO. All rats exhibited severe neurological deficits with a mean score of 2 as assayed on Longa five-point score before the initial treatment.²⁰ During the experimental period, one rat died at 48 h after eMCAO in the saline group (10%), two at 24 h and 48 h, respectively, in the tPA group (20%), two at 24 h and 48 h, respectively, in the sEVs group (20%), and zero in the tPA+sEVs group. Compared to the saline treatment, monotherapy of tPA did not significantly reduce neurological deficits measured with an array of well established behavioral tests, although spontaneous recovery occurred (Figure 1(a)). CEC-sEVs alone also did not significantly improve neurological outcomes (Figure 1(a)). In contrast, CEC-sEVs/tPA significantly reduced neurological deficits and reduced infarct volume by $\sim 40\%$ compared to tPA alone and saline (Figure 1(a) and (c)). The combination of CEC-sEVs with tPA did not significantly increase gross hemorrhage in the ischemic rat compared to saline or monotherapy of tPA (Figure 1(b)).

We then examined the effect of CEC-sEVs on ischemia and reperfusion to mimic thrombectomy in rats subjected to tMCAO. Two out of 8 rats (25%) from the saline group and 1 out of 7 (14%) from the CEC-sEV group died during withdrawal of the

filament and initiation of IA injection. These rats were excluded from experimental data analysis because they died before the treatments. Rats subjected to tMCAO were treated with CEC-sEVs (1×10^{11} particles/rat) via the internal carotid artery (IA) immediately following the withdrawal of the filament at 2 h after MCAO. A second dose of CEC-sEVs was given 24 h later via a tail vein (IV). We found that CEC-sEVs significantly reduced infarct volume by $\sim 37\%$ and improved neurological function compared with saline (Figure 1(d) and (e)). These data indicate that CEC-sEVs adjunctive with tPA initially administered 4 h post eMCAO and CEC-sEVs treatment of tMCAO given upon reperfusion have a therapeutic effect for acute ischemic stroke.

Early intravenous administration of CEC-sEVs suppresses ischemic lesion expansion

The ischemic core expands during the acute ischemic stage, which results in a reduction of the ischemic penumbra.³⁶ To examine whether early administration of CEC-sEVs reduces ischemic core lesion expansion, we administered CEC-sEVs (I.V) to ischemic rats at 1 h after eMCAO and then examined the dynamic expansion of the ischemic lesion 2 and 24 h after eMCAO using ADC and T2 weighted MRI images. CEC-sEVs monotherapy led to ischemic lesion expansion by 38% from $24.3 \pm 2.0\%$ of volume at 2 h to $33.5 \pm 7.0\%$ at 24 h, whereas saline treatment resulted in lesion expansion of 80% from $23.5 \pm 3.0\%$ at 2 h to $42.2 \pm 7.0\%$ at 24 h of eMCAO. The difference in ischemic lesion expansion between these two groups was significant ($p < 0.05$). These data suggest that the early administration of CEC-sEVs attenuates ischemic core lesion expansion, which would preserve a large penumbra and thus may permit more patients to be eligible for tPA and thrombectomy treatments.¹

CEC-sEVs/tPA promotes recanalization, increase CBF and downstream vascular patency, and reduce BBB leakage

To examine the effect of CEC-sEVs/tPA on recanalization of the occluded MCA and its downstream microvascular perfusion, additional experiments were performed on rats with eMCAO. The combination of CEC-sEVs with tPA given 4 h after eMCAO significantly reduced the embolus size at the origin of the occluded MCA compared with tPA monotherapy when the rats were sacrificed at 24 h after eMCAO (Figure 2(a)). To examine downstream non-occluded microvessels, we injected FITC-dextran to the rats via a tail vein at 24 h after eMCAO and sacrificed the rats 15 min after the injection for FITC-plasma to perfuse

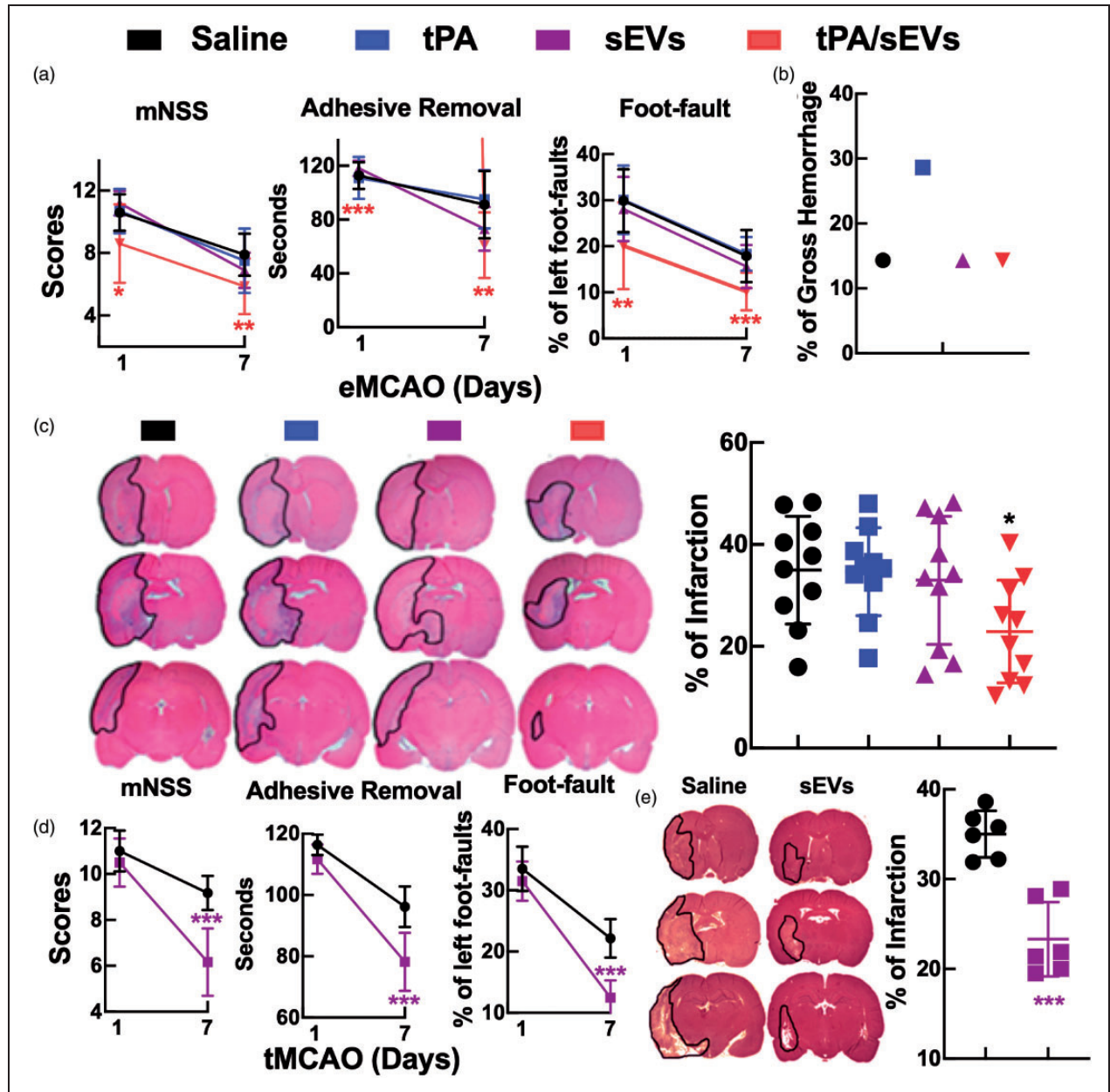


Figure 1. The effects of CEC-sEVs/tPA or CEC-sEVs given upon reperfusion to rats subjected to eMCAO or tMCAO, respectively. The effect of CEC-sEVs/tPA on an array of behavioral tests (A), brain hemorrhage (B), and infarct volume (C) of rats subjected to eMCAO when tPA and/or CEC-sEVs were administered 4 h after eMCAO. Panel C shows representative images of H&E stained brain coronal sections and their quantitative data. $N = 10/\text{group}$, $*p < 0.05$; $**p < 0.01$, and $***p < 0.001$ vs Saline. The effect of CEC-sEVs administered upon reperfusion at 2 h of tMCAO on an array of behavioral tests (D) and infarct volume (E) of rats subjected to tMCAO. $N = 6/\text{group}$, $***p < 0.001$ vs Saline.

all open cerebral vessels.^{23,24,37} 3D LSCM analysis showed that the combination treatment sEVs with tPA given 4 h after eMCAO significantly increased FITC-dextran perfused downstream microvessels (Figure 2(b)). The combination therapy also significantly reduced BBB leakage measured by Evans blue, parenchymal fibrin deposition, and platelet accumulation compared with tPA alone (Figure 2(c) to (e)). MRI

measurement in the same rat before and after the treatment showed that CEC-sEVs/tPA promoted recanalization of the occluded MCA as measured with magnetic resonance angiography, increased downstream CBF measured with perfusion-weighted imaging, and decreased ischemic lesion measured with ADC, and T2²⁴ 24 h after eMCAO compared with tPA monotherapy (Figure 3). Collectively, these data

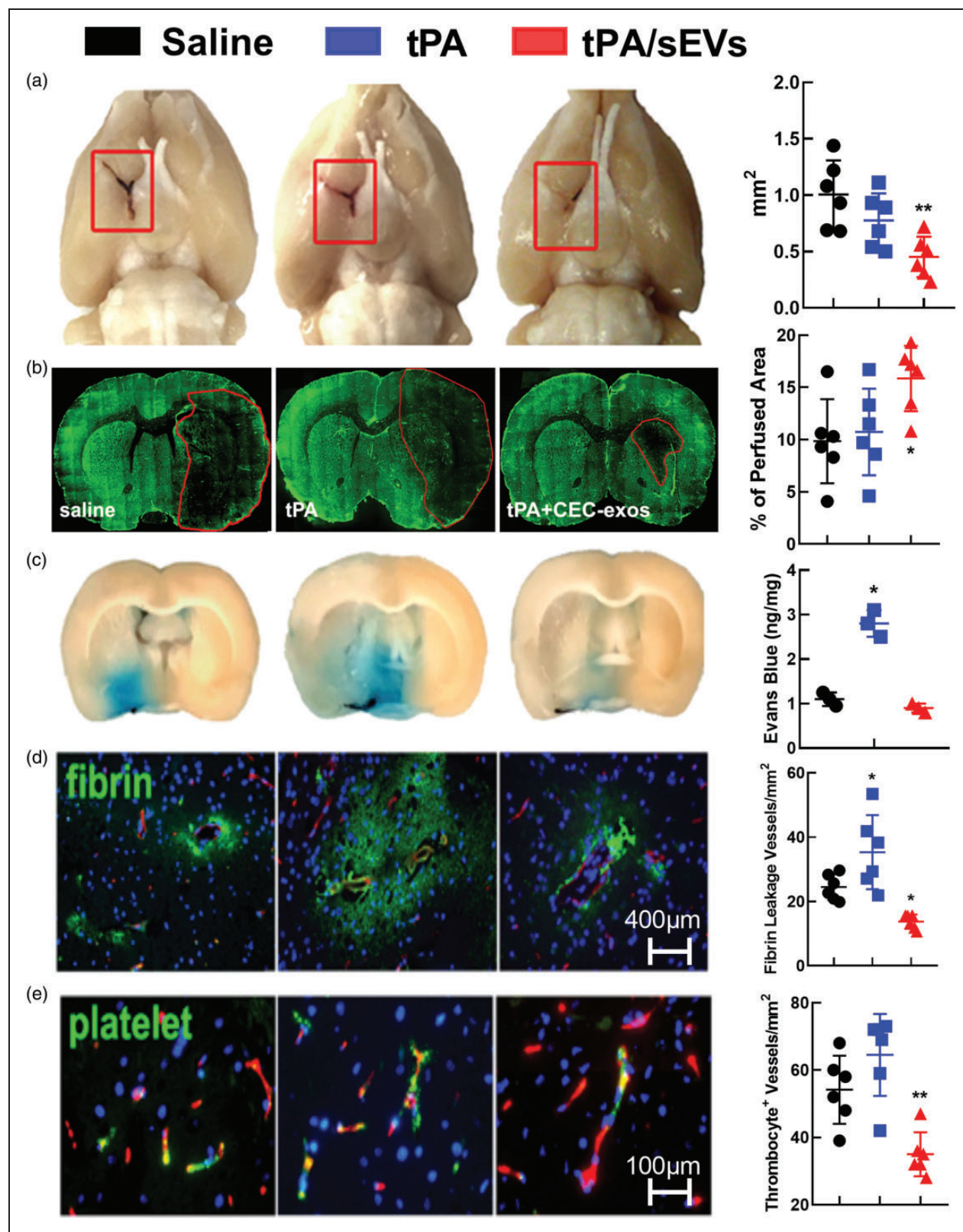


Figure 2. The effect of CEC-sEVs/tPA on thrombosis and BBB leakage. CEC-sEVs/tPA significantly reduced embolus size at the origin of the occluded MCA (A), downstream FITC-plasma-perfused microvessels (B), Evans blue leakage (C), extravascular fibrin deposition assayed by double immunofluorescent staining (D, green), and intravascular platelet aggregation assayed by double immunofluorescent staining (E, green). The red color in panels D and E is EBA immunoreactive vessels. N = 6/group, *p < 0.05 and **p < 0.01 vs Saline.

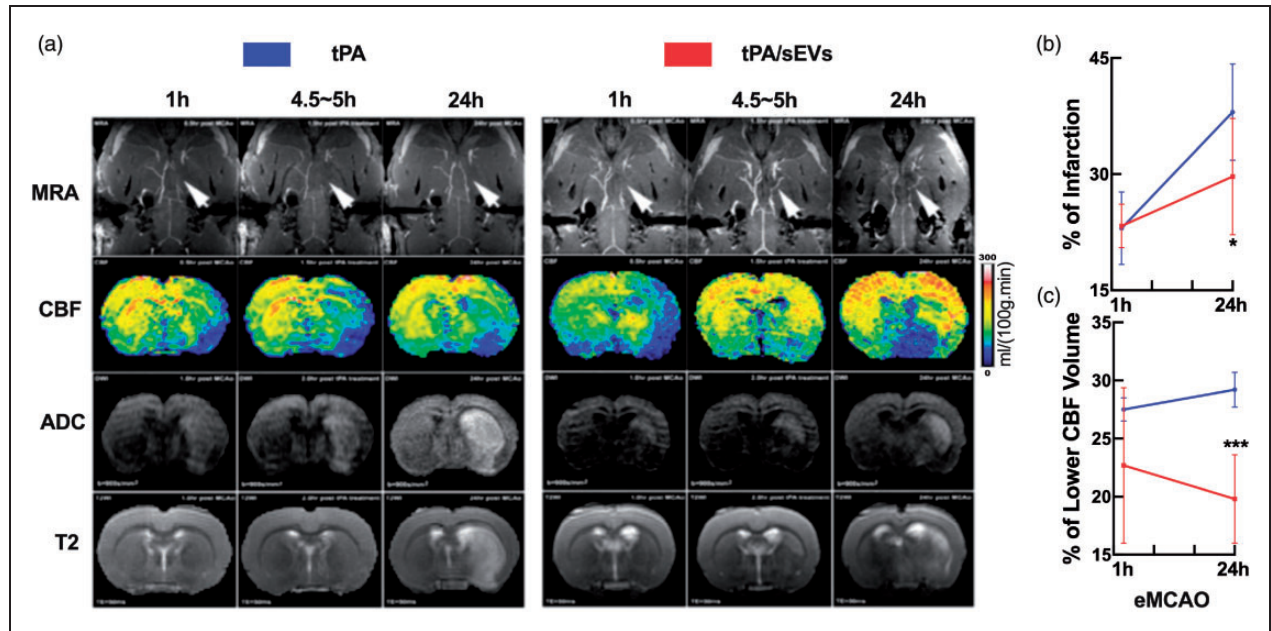


Figure 3. The effect of CEC-sEVs/tPA on recanalization, CBF, and ischemic lesion. Representative MRI images (A) show recanalization of occluded MCA measured by magnetic resonance angiography (MRA, arrow), CBF by perfusion-weighted image, ischemic lesion by ADC and T2 at pre-treatment (1 h), immediately after the treatment (4.5-5 h) and post-treatment (24 h) in representative rats subjected to eMCAO and treated with tPA or treated with tPA in combination with CEC-sEVs (CEC-sEVs/tPA). Panel B shows areas with low CBF and infarct volume measured by T2. N = 6/group, * $p < 0.05$ and *** $p < 0.001$ vs tPA monotherapy.

strongly suggest that CEC-sEVs facilitate tPA-induced thrombolysis of the occluded MCA, increase downstream microvascular reperfusion, and reduce BBB leakage and infarction, which consequently lead to improvements of neurological function.

CEC-sEVs elevate a set of miRs and reduce pro-thrombotic and BBB leakage proteins in CECs

To examine the effect of CEC-sEVs/tPA on miRs, we analyzed miRs in primary CECs isolated from the ischemic blood vessels of rats subjected to 24h eMCAO using qRT-PCR. We found that CECs harvested from ischemic rats treated with saline or tPA exhibited significantly reduced miR-19a, -21, and -146a expression compared with CECs from non-ischemic rats, whereas the endothelial cells from rats treated with CEC-sEVs/tPA did not show a significant reduction of these three miRs compared with CECs from non-ischemic rats (Figure 4(a)). Western blot analysis of the endothelial cells from the same sets of rats showed that compared with non-ischemic, saline or tPA treatment increased levels of TLR4, ICAM-1, PAI-1, TF, and pNF- κ B, and reduced ZO1, which were reversed by the combination CEC-sEVs/tPA treatment (Figure 4(b)). Bioinformatics analysis revealed that the altered miRs and proteins form a network that promotes vascular injury, thrombogenicity, and BBB leakage³⁸⁻⁴⁰ (Figure 4(c)). Using miR arrays,

we analyzed CEC-sEVs cargo miRs and found that miR-19a, -21 and -146a were among the top 10 enriched miRs within CEC-sEVs including miR-328a, -483, -125b, -344a, -211, and let-7b and let-7c. These data suggest that miRs and proteins altered by CEC-sEVs contribute to the therapeutic effect of CEC-sEVs on acute stroke.

To investigate whether the beneficial effects of CEC-sEVs on cerebral endothelial cell function observed after stroke in rodents are present in human CECs and whether human CEC-sEVs provide a vascular therapeutic effect, we isolated sEVs from thrombectomy-retrieved arterial thrombi of patients with acute ischemic stroke. These patient arterial clots derived sEVs had doughnut morphology and a mean diameter of 85.6 ± 1.7 nm assayed by TEM and NTA and showed sEV marker proteins, CD63, and Alix (Figure 5). Using an in vitro trans-endothelial permeability assay,⁴¹ we then examined the effect of patient-clot-derived sEVs on endothelial permeability. Incubating healthy human CECs with patient-clot-derived sEVs significantly increased endothelial cell leakage (Figure 5). Moreover, the clot-derived sEVs substantially reduced endothelial cell miR-19a, -21, and -146a and increased proteins of TLR4, ICAM-1, PAI-1, TF, and NF- κ B (Figure 5). Importantly, the concurrent addition of sEVs derived from healthy human CECs with the clot-derived sEVs significantly

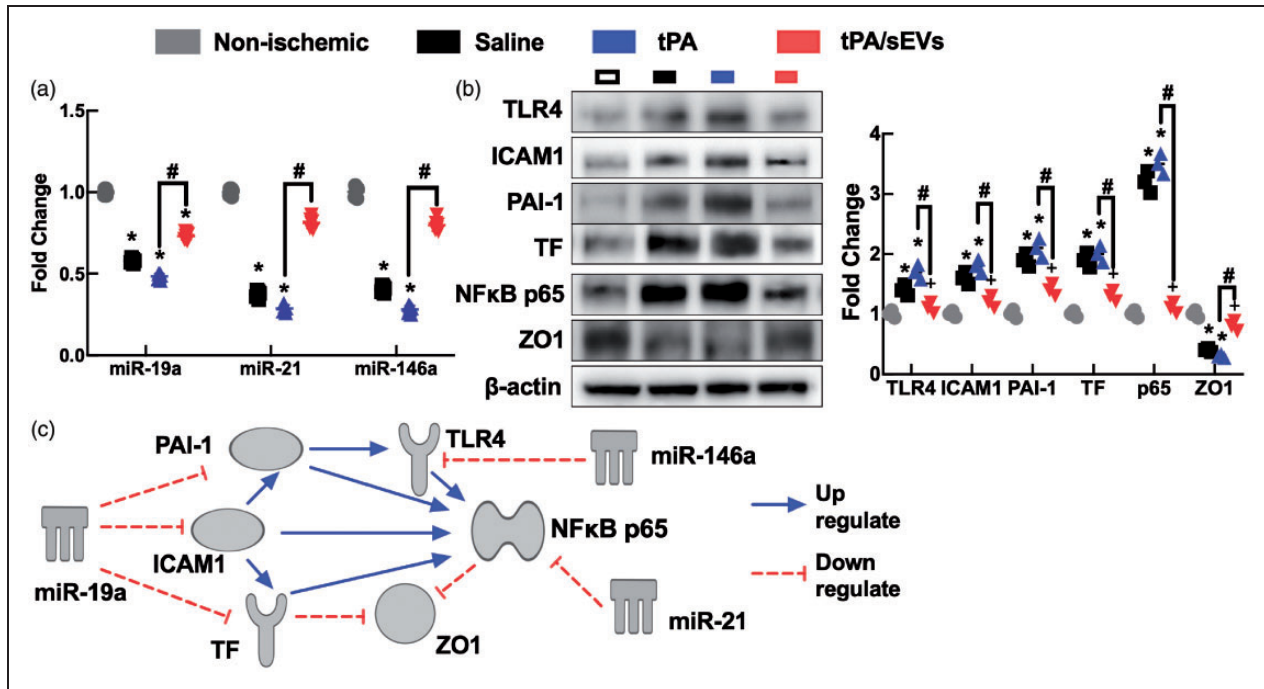


Figure 4. The effect of CEC-sEVs/tPA on cerebral vascular miRs and proteins. CEC-sEVs/tPA significantly upregulated miR-19a, -21, and -146a assayed by qRT-PCR (A). Panel B shows representative Western blot images and their quantitative data of protein levels of TLR4, ICAM1, NF-KB-p65, PAI-I, TF, and ZO-I in rats subjected to eMCAO and treated with saline, tPA alone, and CEC-sEVs/tPA. CECs derived from non-ischemic rats were used as a control. Panel C shows a network of miR-19a, 21, and 146a and their putative target genes generated by IPA. N = 6/group, *p < 0.05 vs Saline and #p < 0.05 vs indicated group.

reduced patient-clot-derived sEV increased endothelial cell leakage and reversed miRs and proteins altered by patient-clot-derived sEVs (Figure 5). These data provide evidence that patient-clot-derived sEVs promote thrombosis and BBB leakage, which can be reduced by healthy human CEC-sEVs.

CEC-sEVs intravenously administered cross the BBB and are internalized by CECs, astrocytes, and neurons

To track the brain distribution of intravenously administered CEC-sEVs, we treated rats subjected to 4 h of eMCAO with CEC-sEVs isolated from healthy CECs transfected with CD63-GFP plasmids (GFP-CEC-sEVs, Figure 6). Confocal microscopic images showed that GFP signals were primarily found in cells lining the cerebral blood vessels and neurons in the ipsilateral hemisphere at 2 h after the IV injection (Figure 6). TEM analysis revealed that GFP-immunogold particles were localized to endothelial cells of cerebral microvessels with intact tight junction, astrocyte foot-processes, and neurons (Figure 6). Omitting the primary antibody against GFP resulted in no detection of GFP-gold particles. These data provide evidence that CEC-sEVs cross the BBB and that astrocytes and

neurons in the ischemic hemisphere can internalize CEC-sEVs.

Discussion

The present study demonstrates that CEC-sEVs either in combination with tPA or given immediately upon reperfusion enhance thrombolysis and recanalization and reduce BBB leakage in a rat model of embolic stroke and reduce cerebral infarction and improve neurological outcomes after both eMCAO and tMCAO, i.e., in rat models of ischemic stroke with a large arterial occlusion. Intravenously administered CEC-sEVs cross the BBB and are internalized by the neural cells in the ischemic brain. CEC-sEVs/tPA substantially increase a set of CEC-sEV cargo-enriched miRs in CECs, and significantly reduce tPA- and ischemia-increased proteins that mediate thrombosis and BBB leakage. Importantly, a therapeutic effect of CEC-sEVs was also observed in human cerebral endothelial cells impaired by patient arterial clot derived sEVs. Together, the present study provides evidence that CEC-sEVs significantly reduce stroke-induced neuro-vascular damage and improve neurological outcomes.

Mechanical endovascular thrombectomy and tPA are now the standards of care for the treatment of patients with acute ischemic stroke who meet inclusion

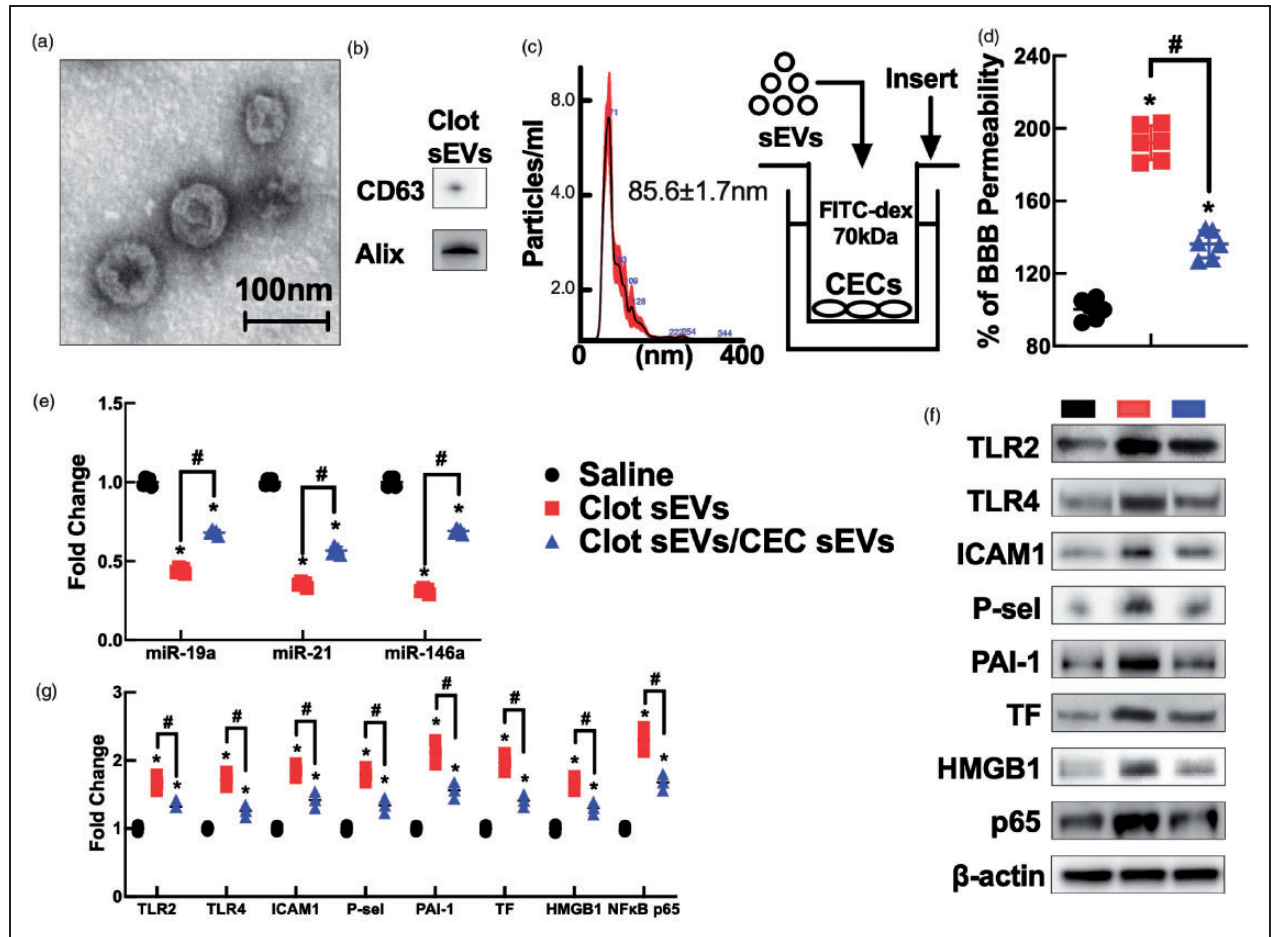


Figure 5. The effect of sEVs derived from arterial clots of patients with acute ischemic stroke on human cerebral endothelial permeability. Representative TEM and Western blot images show that clot derived sEVs have cup-shaped morphology (A), proteins of CD63 and Alix (B), and clot sEVs distribution (C). Panel D shows a schematic cerebral endothelial cell permeability assay and quantitative data of permeability changes in human CECs treated with saline, clot derived sEVs alone (clot-sEVs) or clot derived sEVs with sEVs derived from healthy human cerebral endothelial cells (clot-sEVs/CEC-sEVs), ($n = 6/\text{group}$). Panel E shows qRT-PCR data of miR-19a, -21, and -146a in CECs after the specified treatments, ($n = 5/\text{group}$). Panel F and G show representative Western blot images of individual proteins in CECs and their quantitative data after the specified treatments ($n = 5/\text{group}$). * $p < 0.05$ vs saline and # $p < 0.05$ vs indicated group. P-sel = P-selectin.

criteria.^{1,2,4-8} Patients with timely reperfusion of the ischemic lesion have increased likelihood of achieving good clinical outcomes.^{1,2} Using models of eMCAO in the rhesus macaques, mouse, and rat, recent studies demonstrate that enhancement of reperfusion by tPA in combination with selective intra-arterial cooling and an angiotensin type 2 receptor agonist substantially reduces and improves neurovascular damage and neurological function, respectively.⁴²⁻⁴⁴ We and others previously demonstrated that exosomes derived from mesenchymal stem cells and other cell types enhance brain remodeling during stroke recovery.¹²⁻¹⁴ However, studies that have used sEVs for enhancing brain perfusion after acute ischemic stroke with a large artery occlusion are limited.¹² The present study, for the first time, demonstrates that CEC-sEVs

robustly enhance tPA-induced thrombolysis and robustly reduced BBB leakage and infarction in a model of eMCAO. The evolution of the hypoperfused penumbra to irreversible infarction leads to ischemic core expansion, which results in many patients with large vessel occlusion being not eligible to receive tPA or endovascular therapy.^{2,8} The present study demonstrates that when rats are treated with CEC-sEV monotherapy early (1 h) after the onset of eMCAO, the expansion of the ischemic core is substantially attenuated. Collectively, these data indicate that CEC-sEVs substantially reduce stroke-induced neurovascular damage. The present study also provides the first evidence that sEVs derived from arterial clots of patients with acute ischemic stroke impair cerebral endothelial cell permeability, whereas sEVs derived from healthy

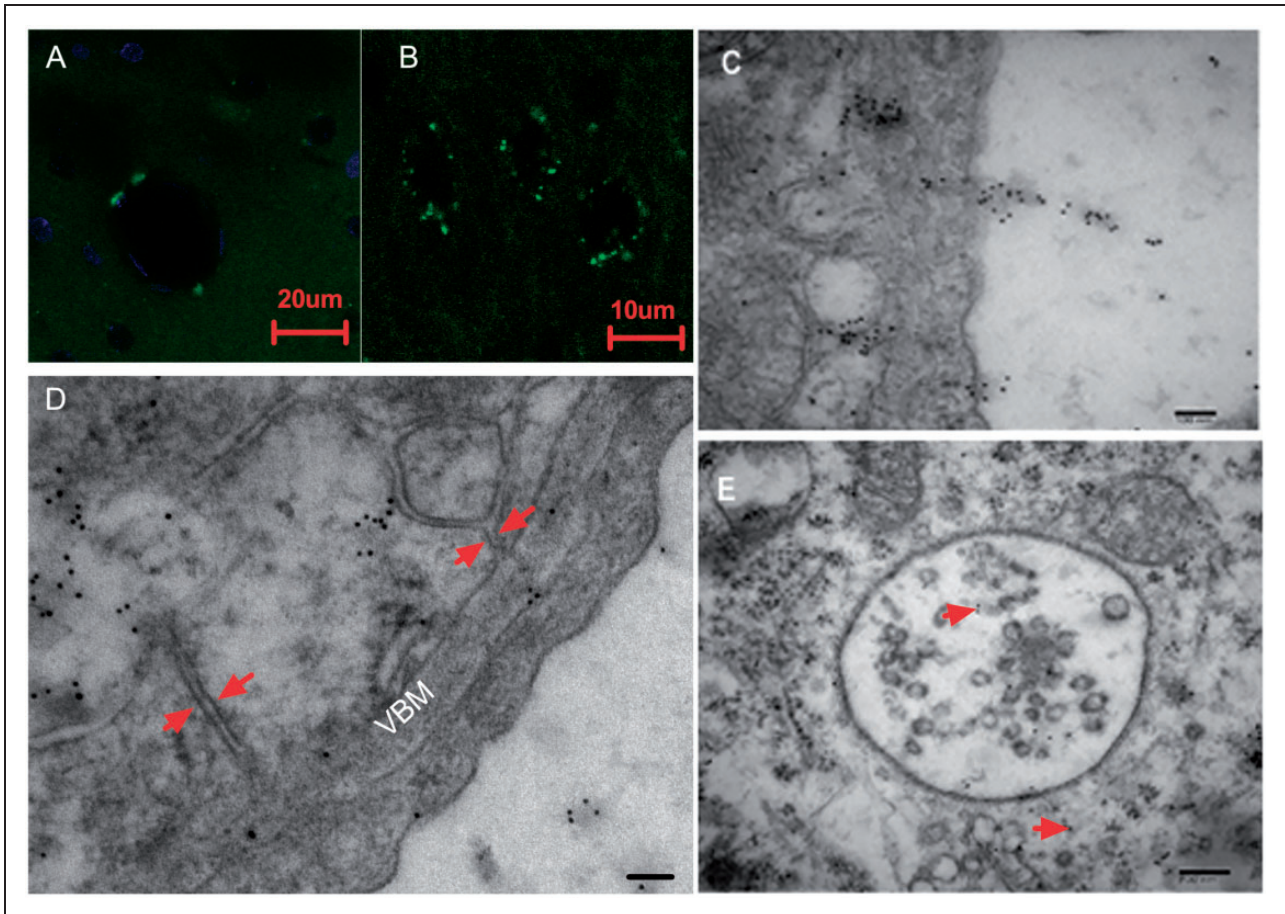


Figure 6. Brain distribution of intravenously administered GFP-CEC-sEVs. Representative orthogonal confocal images showed GFP signals in CECs (A) and neurons (B) after intravenous administration (IV) of GFP-CEC-sEVs. Representative TEM images showed that GFP positive gold particles from cerebral blood vessel lumen crossed endothelial cells and reached astrocyte foot processes (C, D, arrows) and within the cytoplasm and multivesicular body (MVB) of neurons (E, arrows). VBM in D = vascular base membrane. Bars in C = 100 nm, D and E = 200 nm, respectively.

human CECs attenuate the effect of patient clot-derived sEVs on cell permeability. These *in vitro* data suggest that in addition to arterial thrombi, sEVs from the clot damage CECs, and that human CEC-sEVs have a therapeutic effect on injured CECs as do rat CEC-sEVs. Compounds employed for the treatment of acute ischemic stroke need to meet multiple requirements including facilitation of recanalization, enhancement of fibrinolysis and thrombolysis, vascular stabilization, and increase of BBB integrity and amplification of neuroprotection.^{4,6,45} Thus, the treatment with CEC-sEVs as adjunctive therapy with tPA and/or mechanical thrombectomy potentially augment neuroprotection by robustly reducing neurovascular damage of acute ischemic stroke.

EVs can transfer their cargo biological materials including miRs to recipient cells, consequently leading to changes in recipient cell function.^{46,47} The present study shows that the CEC-sEVs/tPA results in the

upregulation of a set of miRs (miR-19a/21/146a), which are inversely associated with protein levels of TLR4, ICAM-1, PAI-1, and TF in CECs. The altered miRs and associated proteins form a network that mediates thrombosis, inflammation, and BBB integrity.^{48,49} Injured endothelial cells upregulate TF, ICAM-1, HMGB1, and P-selection, which amplify vascular injury and thrombogenicity by forming neutrophil extracellular traps (NETs).^{38–40} The TLR signaling pathway mediates cerebral endothelial cell function and regulates the formation of NETs.³⁹ Formation of NETs in the cerebral artery is highly associated with the worse neurological outcomes of patients with acute stroke.⁴⁸ Among miRs, miR-146a is a well characterized miR that targets TLR signaling.^{50,51} We previously demonstrated that elevation of miR-146a in cerebral endothelial cells reduces fibrin-increased cell permeability by targeting TLR2 and TLR4.⁵² MiR-21 also targets TLR4,⁵³ while miR-19 exerts anti-thrombotic

effects by suppressing genes of TF and PAI-1.^{54,55} Importantly, miR-19, -21, and -146a are well conserved between human and rodent.^{54,55} Collectively, the present study suggests that the CEC-sEV cargo miRs likely contribute to the therapeutic effect of CEC-sEVs on the improvement of neurovascular function, which has the potential for clinical translation. However, additional studies are warranted to validate this premise and to investigate the role of CEC-sEV cargo proteins in the observed beneficial effects of CEC-sEVs on acute ischemic stroke.

Our ultrastructural data provide supportive evidence that intravenously administered CEC-sEVs cross the BBB and are internalized by neurons and other parenchymal cells. Localization of CEC-sEVs within astrocyte foot-processes suggests that CEC-sEVs act on astrocytes to improve BBB integrity. Additionally, CEC-sEVs reach injured neurons, which potentially protects ischemic damaged neurons. Thus, in addition to CECs, CEC-sEVs act on astrocytes and neurons, which may contribute to the therapeutic effect of CEC-sEVs on reducing ischemic neurovascular damage. However, further studies are warranted to investigate the contributions of individual cell types to the improved neurological function.

In summary, the present study indicates that CEC-sEVs have a therapeutic effect on acute ischemic stroke in the rat by facilitating recanalization, enhancing fibrinolysis and thrombolysis, enhancing BBB integrity, reducing inflammation, and amplifying neuroprotection.⁴⁵ These data are also of importance in light of recent findings showing that COVID19 patients with acute ischemic stroke had robust thrombosis, inflammation, and worse stroke outcome.^{56–59}

Funding

The author(s) disclosed receipt of the following financial support for the research, authorship, and/or publication of this article: This work was supported by grants from NIH RO1 NS111801 for ZG, Zhang, and NIH R56 AG055583 for L, Zhang.

Acknowledgments

The authors thank Amy Kemper for TEM.

Declaration of conflicting interests

The author(s) declared no potential conflicts of interest with respect to the research, authorship, and/or publication of this article.

Authors' contributions

CL and ZG conceived and designed the study; CW, YZ, OA, AC, SM, ML, MK, HM, GD, QJ, and LZ contributed to data acquisition, analysis and interpretation; CL and ZG

drafted the manuscript; MC and ZG approved the manuscript for submission.

ORCID iD

Chao Li  <https://orcid.org/0000-0001-9629-9219>

Supplemental material

Supplemental material for this article is available online.

References

1. Goyal M, Hill MD, Saver JL, et al. Challenges and opportunities of endovascular stroke therapy. *Ann Neurol* 2016; 79: 11–17.
2. Saver JL, Goyal M, van der Lugt A, et al.; HERMES Collaborators. Time to treatment with endovascular thrombectomy and outcomes from ischemic stroke: a meta-analysis. *Jama* 2016; 316: 1279–1288.
3. Tissue plasminogen activator for acute ischemic stroke. *N Engl J Med* 1995; 333: 1581–1587.
4. Catanese L, Tarsia J and Fisher M. Acute ischemic stroke therapy overview. *Circ Res* 2017; 120: 541–558.
5. Fisher M and Saver JL. Future directions of acute ischemic stroke therapy. *Lancet Neurol* 2015; 14: 758–767.
6. Neuhaus AA, Couch Y, Hadley G, et al. Neuroprotection in stroke: the importance of collaboration and reproducibility. *Brain* 2017; 140: 2079–2092.
7. Jadhav AP, Desai SM, Kenmuir CL, et al. Eligibility for endovascular trial enrollment in the 6- to 24-hour time window: analysis of a single comprehensive stroke center. *Stroke* 2018; 49: 1015–1017.
8. Ganesh A and Goyal M. Thrombectomy for acute ischemic stroke: recent insights and future directions. *Curr Neurol Neurosci Rep* 2018; 18: 59–07.
9. Goyal M, Demchuk AM, Menon BK, et al. Randomized assessment of rapid endovascular treatment of ischemic stroke. *N Engl J Med* 2015; 372: 1019–1030.
10. Zhang ZG and Chopp M. Exosomes in stroke pathogenesis and therapy. *J Clin Invest* 2016; 126: 1190–1197.
11. Marcus ME and Leonard JN. FedExosomes: engineering therapeutic biological nanoparticles that truly deliver. *Pharmaceuticals (Basel)* 2013; 6: 659–680.
12. Xin H, Li Y, Cui Y, et al. Systemic administration of exosomes released from mesenchymal stromal cells promote functional recovery and neurovascular plasticity after stroke in rats. *J Cereb Blood Flow Metab* 2013; 33: 1711–1715.
13. Xin H, Li Y, Buller B, et al. Exosome-mediated transfer of miR-133b from multipotent mesenchymal stromal cells to neural cells contributes to neurite outgrowth. *Stem Cells* 2012; 30: 1556–1564.
14. Zhang Y, Chopp M, Meng Y, et al. Effect of exosomes derived from multipotent mesenchymal stromal cells on functional recovery and neurovascular plasticity in rats after traumatic brain injury. *JNS* 2015; 122: 856–867.
15. Lapchak PA, Boitano PD, de Couto G, et al. Intravenous xenogeneic human cardiosphere-derived cell extracellular vesicles (exosomes) improves behavioral function in

- small-clot embolized rabbits. *Exp Neurol* 2018; 307: 109–117.
16. Brennan K, Martin K, FitzGerald SP, et al. A comparison of methods for the isolation and separation of extracellular vesicles from protein and lipid particles in human serum. *Sci Rep* 2020; 10: 1039.
 17. Vella LJ, Scicluna BJ, Cheng L, et al. A rigorous method to enrich for exosomes from brain tissue. *J Extracell Vesicles* 2017; 6: 1348885–1348885.
 18. Powers WJ, Rabinstein AA, Ackerson T, et al. Guidelines for the early management of patients with acute ischemic stroke: 2019 update to the 2018 guidelines for the early management of acute ischemic stroke: a guideline for healthcare professionals from the American Heart Association/American Stroke Association. *Stroke* 2019; 50: e344–e418.
 19. Zhang RL, Chopp M, Zhang ZG, et al. A rat model of focal embolic cerebral ischemia. *Brain Res* 1997; 766: 83–92.
 20. Longa EZ, Weinstein PR, Carlson S, et al. Reversible middle cerebral artery occlusion without craniectomy in rats. *Stroke* 1989; 20: 84–91.
 21. Jiang Q, Zhang ZG, Zhang RL, et al. Diffusion, perfusion, and T2 magnetic resonance imaging of anti-intercellular adhesion molecule 1 antibody treatment of transient Middle cerebral artery occlusion in rat. *Brain Res* 1998; 788: 191–201.
 22. Jiang Q, Zhang RL, Zhang ZG, et al. Magnetic resonance imaging indexes of therapeutic efficacy of recombinant tissue plasminogen activator treatment of rat at 1 and 4 hours after embolic stroke. *J Cereb Blood Flow Metab* 2000; 20: 21–27.
 23. Zhang L, Zhang RL, Jiang Q, et al. Focal embolic cerebral ischemia in the rat. *Nat Protoc* 2015; 10: 539–547.
 24. Ding G, Jiang Q, Li L, et al. MRI of combination treatment of embolic stroke in rat with rtPA and atorvastatin. *J Neurol Sci* 2006; 246: 139–147.
 25. Zhang Z, Zhang L, Yepes M, et al. Adjuvant treatment with neuroserpin increases the therapeutic window for tissue-type plasminogen activator administration in a rat model of embolic stroke. *Circulation* 2002; 106: 740–745.
 26. Jiang Q, Zhang RL, Zhang ZG, et al. Magnetic resonance imaging characterization of hemorrhagic transformation of embolic stroke in the rat. *J Cereb Blood Flow Metab* 2002; 22: 559–568.
 27. Zhang L, Zhang ZG, Zhang C, et al. Intravenous administration of a GPIIb/IIIa receptor antagonist extends the therapeutic window of intra-arterial tenecteplase-tissue plasminogen activator in a rat stroke model. *Stroke* 2004; 35: 2890–2895.
 28. Schaar KL, Brennenman MM and Savitz SI. Functional assessments in the rodent stroke model. *Exp Transl Stroke Med* 2010; 2: 13.
 29. Schallert T and Whishaw IQ. Bilateral cutaneous stimulation of the somatosensory system in hemidecorticate rats. *Behav Neurosci* 1984; 98: 518–540.
 30. Hua Y, Schallert T, Keep RF, et al. Behavioral tests after intracerebral hemorrhage in the rat. *Stroke* 2002; 33: 2478–2484.
 31. Jiang Q, Ewing JR, Ding GL, et al. Quantitative evaluation of BBB permeability after embolic stroke in rat using MRI. *J Cereb Blood Flow Metab* 2005; 25: 583–592.
 32. Li C, Zhang Y, Levin AM, et al. Distal axonal proteins and their related MiRNAs in cultured cortical neurons. *Mol Neurobiol* 2019; 56: 2703–2713.
 33. Li C, Zhang L, Wang C, et al. N-acetyl-seryl-aspartyl-lysyl-proline augments thrombolysis of tPA (tissue-type plasminogen activator) in aged rats after stroke. *Stroke* 2019; 50: 2547–2554.
 34. Wang L, Chopp M, Szalad A, et al. Exosomes derived from Schwann cells ameliorate peripheral neuropathy in type 2 diabetic mice. *Diabetes* 2020; 69: 749–759.
 35. Kowal J, Arras G, Colombo M, et al. Proteomic comparison defines novel markers to characterize heterogeneous populations of extracellular vesicle subtypes. *Proc Natl Acad Sci USA* 2016; 113: E968–977.
 36. Leigh R, Knutsson L, Zhou J, et al. Imaging the physiological evolution of the ischemic penumbra in acute ischemic stroke. *J Cereb Blood Flow Metab* 2018; 38: 1500–1516.
 37. Zhang ZG, Zhang L, Jiang Q, et al. VEGF enhances angiogenesis and promotes blood-brain barrier leakage in the ischemic brain. *J Clin Invest* 2000; 106: 829–838.
 38. Gouloupoulou S, McCarthy CG and Webb RC. Toll-like receptors in the vascular system: sensing the dangers within. *Pharmacol Rev* 2016; 68: 142–167.
 39. Papayannopoulos V. Neutrophil extracellular traps in immunity and disease. *Nat Rev Immunol* 2018; 18: 134–147.
 40. McEver RP. Selectins: initiators of leucocyte adhesion and signalling at the vascular wall. *Cardiovasc Res* 2015; 107: 331–339.
 41. Niego B, Freeman R, Puschmann TB, et al. t-PA-specific modulation of a human blood-brain barrier model involves plasmin-mediated activation of the rho kinase pathway in astrocytes. *Blood* 2012; 119: 4752–4761.
 42. Ishrat T, Fouda AY, Pillai B, et al. Dose-response, therapeutic time-window and tPA-combinatorial efficacy of compound 21: a randomized, blinded preclinical trial in a rat model of thromboembolic stroke. *J Cereb Blood Flow Metab* 2019; 39: 1635–1647.
 43. Wang R, Wang H, Liu Y, et al. Optimized mouse model of embolic MCAO: From cerebral blood flow to neurological outcomes. *J Cereb Blood Flow Metab*. Epub ahead of print 20 April 2020. DOI: 10.1177/0271678X20917625
 44. Wu D, Chen J, Hussain M, et al. Selective intra-arterial brain cooling improves long-term outcomes in a non-human primate model of embolic stroke: efficacy depending on reperfusion status. *J Cereb Blood Flow Metab* 2020; 40: 1415–1426.
 45. Eilaghi A, Brooks J, d'Esterre C, et al. Reperfusion is a stronger predictor of good clinical outcome than recanalization in ischemic stroke. *Radiology* 2013; 269: 240–248.
 46. Mathivanan S, Ji H and Simpson RJ. Exosomes: extracellular organelles important in intercellular communication. *J Proteomics* 2010; 73: 1907–1920.
 47. Simons M and Raposo G. Exosomes – vesicular carriers for intercellular communication. *Curr Opin Cell Biol* 2009; 21: 575–581.

48. Novotny J, Oberdieck P, Titova A, et al. Thrombus NET content is associated with clinical outcome in stroke and myocardial infarction. *Neurology* 2020; 94: e2346–e2360.
49. Mirzaei H, Momeni F, Saadatpour L, et al. MicroRNA: relevance to stroke diagnosis, prognosis, and therapy. *J Cell Physiol* 2018; 233: 856–865.
50. Taganov KD, Boldin MP, Chang KJ, et al. NF-kappaB-dependent induction of microRNA miR-146, an inhibitor targeted to signaling proteins of innate immune responses. *Proc Natl Acad Sci U S A* 2006; 103: 12481–12486.
51. Saba R, Sorensen DL and Booth SA. MicroRNA-146a: a dominant, negative regulator of the innate immune response. *Front Immunol* 2014; 5: 578.
52. Zhang L, Chopp M, Liu X, et al. Combination therapy with VELCADE and tissue plasminogen activator is neuroprotective in aged rats after stroke and targets microRNA-146a and the toll-like receptor signaling pathway. *Arterioscler Thromb Vasc Biol* 2012; 32: 1856–1864.
53. Xue X, Qiu Y and Yang HL. Immunoregulatory role of microRNA-21 in macrophages in response to bacillus calmette-guerin infection involves modulation of the TLR4/MyD88 signaling pathway. *Cell Physiol Biochem* 2017; 42: 91–102.
54. Teruel R, Perez-Sanchez C, Corral J, et al. Identification of miRNAs as potential modulators of tissue factor expression in patients with systemic lupus erythematosus and antiphospholipid syndrome. *J Thromb Haemost* 2011; 9: 1985–1992.
55. Li S, Ren J, Xu N, et al. MicroRNA-19b functions as potential anti-thrombotic protector in patients with unstable angina by targeting tissue factor. *J Mol Cell Cardiol* 2014; 75: 49–57.
56. Markus HS and Brainin M. COVID-19 and stroke – a global world stroke organization perspective. *Int J Stroke* 2020; 15: 361–364.
57. Trejo-Gabriel-Galán JM. Stroke as a complication and prognostic factor of COVID-19. *Neurologia* 2020; 35: 318–322.
58. Beyrouti R, Adams ME, Benjamin L, et al. Characteristics of ischaemic stroke associated with COVID-19. *J Neurol Neurosurg Psychiatry* 2020; 91: 889–891.
59. Pons S, Fodil S, Azoulay E, et al. The vascular endothelium: the cornerstone of organ dysfunction in severe SARS-CoV-2 infection. *Crit Care* 2020; 24: 353.